arXiv:1612.01982v1 [physics.comp-ph] 6 Dec 2016

An Accurate Globally Conservative Subdomain Discontinuous Least-squares Scheme for Solving Neutron Transport Problems

Weixiong Zheng[a,*], Ryan G. McClarren[a], Jim E. Morel[a]

[a]*Nuclear Engineering, Texas A&M University, College Station, TX 77843-3133*

Abstract

In this work, we present a subdomain discontinuous least-squares (SDLS) scheme for neutronics problems. Ordinary least-squares (LS) method is known to be erroneous in problems with material interfaces that have total cross section sharp changes on two sides. In addition, least-squares scheme is known not to be globally conservative in heterogeneous problems. In problems where global conservation is important, e.g. k-eigenvalue problems, conservative treatment must be applied. We, in this study, proposed a SDLS method that retains global conservation. Such a method resembles LS formulation in each subdomain without material interface and differs from LS that an additional least-squares interface term appears for each interface. Scalar flux is continuous in each subdomain with continuous finite element method (cfem) while discontinuous on interfaces for every pair of contiguous subdomains.

Keywords: Global conservation; least-squares; discrete ordinates

1. Introduction

Neutral particle transport problems are governed by a first-order, hyperbolic equation. As a result particle transport problems, especially those that are streaming dominated, can have discontinuous solutions. Such problems re-

*Corresponding author

Email addresses: zwxne2010@gmail.com (Weixiong Zheng), rgm@tamu.edu (Ryan G. McClarren), morel@tamu.edu (Jim E. Morel)

quire spatial discretizations that allow for discontinuities in space. Moreover, in regions where there is a strong scattering, discontinuous finite elements have been shown to properly preserve the asymptotic diffusion limit of the transport equation [1]. These two facts have led to discontinuous Galerkin finite elements being widely used in transport calculations. Nevertheless, the discontinuous finite element methods have more degrees of freedom than their continuous counterparts, especially in 3-D.

Another approach to solving transport problems involves forming a second-order transport operator, and solving the resulting equations using continuous finite elements. Second-order transport problems based on the parity of the equations and the self-adjoint angular flux (SAAF) equation are well-known[2, 3, 4, 5, 6]. The resulting equations are symmetric, but are ill-posed in void regions and ill-conditioned in near voids.

More recently, Hansen, et al. [7] derived a second-order form that is equivalent to minimizing the squared residual of the transport operator; it is therefore called the least-squares transport equation (LSTE). This method can also be formed by multiplying the transport equation by the adjoint transport operator or by applying least-squares finite elements in space to the transport equation. The resulting equations are well-posed in void and are symmetric positive definite. The least-squares method has previously been investigated in the computational fluid dynamics (CFD) community for a long time[8, 9, 10]. However, such the method generally has low accuracy in problems with interfaces between optically thin and thick materials without local refinement near the interface[11, 12, 13]. Additionally, the standard least-squares method does not have particle conservation (except in the limit as the number of zones goes to infinity), which is a problem in eigenvalue calculations for neutron transport in nuclear systems [14], unless special iteration techniques are applied [15].

In the process of deriving the least-squares equations, the symmetrization of the transport equation converts a hyperbolic equation to an elliptic equation and, in the process, loses causality. For example, the presence of a strong absorber downstream of a source can influence the solution upstream of the

source. In remedying this deficiency, we have to add back in asymmetry to the operator, but do so in such a way that still preserves the positive properties of the least-squares method.

To this end we develop a least-squares method that uses minimizes the square of the transport residual over certain regions of the entire problem domain. In each of these subregions the interaction cross-sections are slowly varying functions of space. We allow the solution between these regions to be discontinuous. The resulting scheme is essentially solves least-squares independently in each subregion, and the regions are coupled through a sweep-like procedure. Furthermore, with the correct weighting in the least-squares procedure, we can construct a method that is globally conservative.

The reminder of the paper is organized as follows: in Sec. 3, we propose a new method that is based on a least-squares formulation over contiguous blocks in the problem base on a novel subdomain-discontinuous functional. We also derive the corresponding weak formulations in this section. Next, we further theoretically demonstrate the method, unlike standard least-squares methods, retains conservation on both a global and subdomain sense. In Sec. 4, several numerical tests are presented to demonstrate conservation as well as the improved accuracy.

2. Revisit least-squares discretization of transport equation

2.1. One group transport equation

We will consider steady, energy-independent transport problems with isotropic scattering in this work. The complications of energy dependence and anisotropic scattering can be readily incorporated into our method. The steady transport equation used to describe neutral particles of a single speed is expressed in operator form as:

$$L\psi = q_{\mathrm{s}}, \tag{1a}$$

where the streaming and removal operator is

$$L = \vec{\Omega} \cdot \nabla(\cdot) + \sigma_{\mathrm{t}}, \quad \text{and} \quad q_{\mathrm{s}} = S\psi + q(\vec{r}, \vec{\Omega}). \tag{1b}$$

In these equations $\psi(\vec{r}, \vec{\Omega})$ is the angular flux of neutrons with units of particles per unit area per unit time, where $\vec{r} \in \mathbb{R}^3$ and $\vec{\Omega} \in \mathbb{S}_2$ is a point on the unit sphere representing a direction of travel for the particles. S is the scattering operator. For isotropic scattering, it is defined as

$$S\psi = \int_{4\pi} d\Omega' \ \sigma_{\mathrm{s}}(\vec{\Omega} \cdot \vec{\Omega}')\psi(\vec{r}, \vec{\Omega}') = \frac{\sigma_{\mathrm{s}}\phi}{4\pi},$$

q is the volumetric source and ϕ is the scalar flux defined as $\phi = \int_{4\pi} d\Omega \ \psi$. Additionally, σ_{t} and σ_{s} are total and scattering cross sections, respectively.

The boundary conditions for Eq. (1) specify the angular flux ψ^{inc} on the boundary for incoming directions:

$$\psi(\vec{r}, \vec{\Omega}) = \psi^{\mathrm{inc}}(\vec{r}, \vec{\Omega}) \qquad \text{for} \quad r \in \partial\mathcal{D}, \qquad \vec{n} \cdot \vec{\Omega} < 0. \tag{2}$$

2.2. LS weak formulation

In order to employ CFEM to solve the transport equation, Hansel, et al. [7] derived a least-squares form of transport equation by multiplying the transport equation by adjoint streaming and removal operator, i.e.

$$L^{\dagger}\left(L\psi - q_{\mathrm{s}}\right) = 0, \tag{3}$$

where

$$L^{\dagger} = -\vec{\Omega} \cdot \nabla(\cdot) + \sigma_{\mathrm{t}}.$$

The corresponding weak form of the problem in Eq. (3) with CFEM is: find $\psi \in \mathcal{V}$ such that $\forall v \in \mathcal{V}$:

$$\oint_{4\pi} d\Omega \int_{\mathcal{D}} dV \ vL^{\dagger}\left(L\psi - q_{\mathrm{s}}\right) = 0, \tag{4}$$

where $\mathcal{D}$ represents the problem domain. The property of adjoint operators that $(Lv, u) = (v, L^{\dagger}u)$, for an inner-product $(\cdot\cdot)$, allows us to express Eq. (4) as

$$\oint_{4\pi} d\Omega \int_{\mathcal{D}} dV \ Lv\left(L\psi - q_{\mathrm{s}}\right) = 0. \tag{5}$$

On the other hand, one could also derive the weak form from defining a least-squares functional of transport residual:

$$\Gamma_{\mathrm{LS}} = \frac{1}{2} \oint_{4\pi} d\Omega \int_{\mathcal{D}} dV \ (L\psi - q_{\mathrm{s}})^2. \tag{6}$$

Minimizing Eq. (6) in a discrete function space $\mathcal{V}$ leads to Eq. (5) as well[1].

2.3. Imposing boundary condition

The derivation above shows ignored the incident boundary conditions. Though it is possible to impose a strong boundary condition [5], a weak boundary condition is chosen in this work instead. To weakly impose the boundary condition, the functional is changed to

$$\Gamma_{\mathrm{LS}} = \frac{1}{2} \oint_{4\pi} d\Omega \int_{\mathcal{D}} dV \ (L\psi - q_{\mathrm{s}})^2 + \frac{1}{2} \int_{\vec{n}\cdot\vec{\Omega}<0} d\Omega \int_{\partial\mathcal{D}} ds \ \lambda \left(\psi - \psi^{\mathrm{inc}}\right)^2, \tag{7}$$

where λ is freely-chosen. The resulting LS weak formulation with boundary condition is then expressed as:

$$\begin{aligned} &\oint_{4\pi} d\Omega \int_{\mathcal{D}} dV \ Lv \left(L - S\right) \psi + \int_{\vec{n}\cdot\vec{\Omega}<0} d\Omega \int_{\partial\mathcal{D}} ds \ \lambda v \psi \\ &\quad = \oint_{4\pi} d\Omega \int_{\mathcal{D}} dV \ Lvq + \int_{\vec{n}\cdot\vec{\Omega}<0} d\Omega \int_{\partial\mathcal{D}} ds \ \lambda v \psi^{\mathrm{inc}}, \end{aligned} \tag{8}$$

where the weight function v is any element of the trial space.

If we choose $\lambda = \sigma_{\mathrm{t}} \left|\vec{n} \cdot \vec{\Omega}\right|$, then in non-void situations the LS scheme is globally conservative in homogeneous media (i.e., where σ_{t} is spatially independent in the whole domain). This can be seen by taking the weight function v to be 1 in Eq. (8) and performing the integration over angle to get

$$\sigma_{\mathrm{t}} \mathbf{B} = 0, \tag{9a}$$

[1]The procedure of the minimization is to find a stationary "point" in specific function space, see Ref. [16] for details

$$\mathbf{B} := \left(\int_{\partial\mathcal{D}} ds\ j^{\text{out}} - \int_{\vec{n}\cdot\vec{\Omega}<0} d\Omega \int_{\partial\mathcal{D}} ds\ \left|\vec{n}\cdot\vec{\Omega}\right| \psi^{\text{inc}} + \int_{\mathcal{D}} dV(\sigma_{\text{a}}\phi - Q) \right), \quad (9b)$$

$$j^{\text{out}} := \int_{\vec{n}\cdot\vec{\Omega}>0} d\Omega\ \left|\vec{n}\cdot\vec{\Omega}\right| \psi \quad \text{and} \quad Q := \int_{4\pi} d\Omega\ q. \quad (9c)$$

Here $\mathbf{B}$ is the global balance: it states that the outgoing current, j^{out}, plus the absorption $\sigma_{\text{a}}\phi$ is equal to the total source plus the incoming current. These equations also demonstrate that why LS cannot maintain conservation in void: when $\sigma_{\text{t}} = 0$, $\mathbf{B}$ becomes undetermined.

3. A least-squares discretization allowing discontinuity on subdomain interface

3.1. The SDLS functional and weak formulation

Given that LS is conservative when the cross-sections are constant and non-void, we propose to reformulate the problem to solve using least-squares in subdomains where cross-sections are constant. On the boundary of these subdomains we connect the angular fluxes using an interface condition that allows the fluxes to be discontinuous. The result is a discretization that can be solved using a procedure analogous to transport sweeps where the sweeps are over subdomains, instead of mesh zones.

In context of a minimization problem, we can define a functional in the following form:

$$\Gamma_{\text{SDLS}} = \frac{1}{2}\sum_{\mathcal{D}_{\text{i}}} \oint_{4\pi} d\Omega \int_{\mathcal{D}_{\text{i}}} dV\ (L_{\text{i}}\psi_{\text{i}} - q_{\text{si}})^2 + \frac{1}{2}\int_{\vec{n}\cdot\vec{\Omega}<0} d\Omega \int_{\partial\mathcal{D}} dV\ \sigma_{\text{t}} \left|\vec{n}\cdot\vec{\Omega}\right| (\psi - \psi^{\text{inc}})^2$$
$$+ \frac{1}{2}\sum_{\mathcal{D}_{\text{i}}}\sum_{\mathcal{F}_{\text{ij}}} \int_{\vec{n}_{\text{i}}\cdot\vec{\Omega}<0} d\Omega \int_{\mathcal{F}_{\text{ij}}} ds\ \sigma_{\text{ti}} \left|\vec{n}_{\text{i}}\cdot\vec{\Omega}\right| (\psi_{\text{i}}^{\text{inc}} - \psi_{\text{j}}^{\text{inc}})^2, \quad (10)$$

where $\mathcal{F}_{\text{ij}}$ is the interface between $\mathcal{D}_{\text{i}}$ and any contiguous subdomain $\mathcal{D}_{\text{j}}$. Accordingly, the variational problem turns to: find ψ_{i} in a polynomial space $\mathcal{V}$

such that $\forall v_\mathrm{i} \in \mathcal{V}$,

$$\sum_{\mathcal{D}_\mathrm{i}} \left(\oint_{4\pi} d\Omega \int_{\mathcal{D}_\mathrm{i}} dV \; L_\mathrm{i} v_\mathrm{i} \left(L_\mathrm{i} - S_\mathrm{i} \right) \psi_\mathrm{i} + \sum_{\mathcal{F}_\mathrm{ij}} \sigma_\mathrm{ti} \int_{\vec{n}_\mathrm{i}\cdot\vec{\Omega}<0} d\Omega \int_{\mathcal{F}_\mathrm{ij}} ds \; \left| \vec{n}_\mathrm{i} \cdot \vec{\Omega} \right| v_\mathrm{i} \left(\psi_\mathrm{i} - \psi_\mathrm{j} \right) \right)$$
$$+ \int_{\vec{n}\cdot\vec{\Omega}<0} d\Omega \oint_{\partial\mathcal{D}} ds \, \sigma_\mathrm{t} \left| \vec{n} \cdot \vec{\Omega} \right| v\psi = \sum_{\mathcal{D}_\mathrm{i}} \oint_{4\pi} d\Omega \int_{\mathcal{D}_\mathrm{i}} dV L_\mathrm{i} v_\mathrm{i} q_\mathrm{i} + \int_{\vec{n}\cdot\vec{\Omega}<0} d\Omega \oint_{\partial\mathcal{D}} ds \, \sigma_\mathrm{t} \left| \vec{n} \cdot \vec{\Omega} \right| v\psi^\mathrm{inc}. \tag{11}$$

Compared with ordinary LS method as illustrated in Eq. (8), SDLS does not enforce the continuity on subdomain interface. That presents possibility of combining the least-squares method and transport sweeps. For a given direction, $\vec{\Omega}$, Eq. (11) can be written as a block-lower triangular system, where each block is LS applied to a subdomain.The inversion of this system requires solving a LS system for each subdomains, connected via boundary angular fluxes. For unstructured meshes this approach can be superior to standard transport sweeps due to potential sweeping and parallel efficiencies.

3.2. Subdomain-wise and global conservation

We can demonstrate that SDLS is conservative globally and over each subdomain.

A conservative scheme with appropriate boundary conditions is expected to retain zero balance, i.e.,

$$\int_{\vec{n}\cdot\vec{\Omega}>0} d\Omega \oint_{\partial\mathcal{D}} ds \, |\vec{n}\cdot\vec{\Omega}|\psi - \int_{\vec{n}\cdot\vec{\Omega}<0} d\Omega \oint_{\partial\mathcal{D}} ds \, |\vec{n}\cdot\vec{\Omega}|\psi^\mathrm{inc} + \int_{\mathcal{D}} dV \, (\sigma_\mathrm{a}\phi - Q) = 0, \tag{12}$$

where $Q = \int_{4\pi} d\Omega \; q$.

To simplify the demonstration, we consider a 1-D slab with only two subdomains (see Figure 1), within each the cross sections are constants. Consequently,

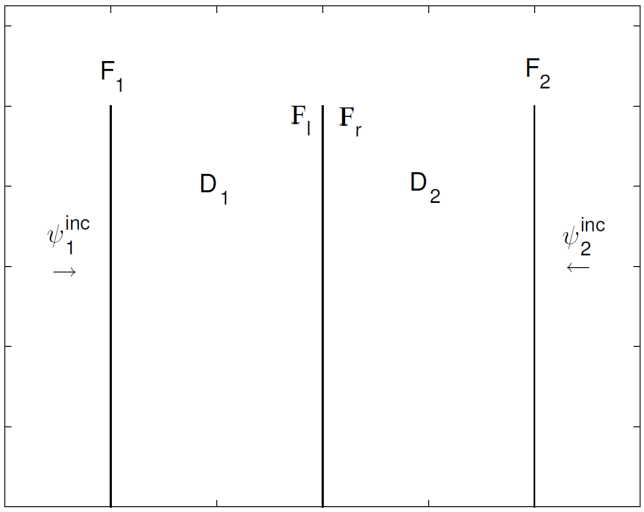

Figure 1: Generic multi-region problem for illustration of global conservation for SDLS.

Eq. (11) with $v_i = 1$ becomes

$$\oint_{4\pi} d\Omega \int_{\mathcal{D}_1} dV\ \sigma_{t1}((L_1 - S_1)\psi_1 - q_1) + \int_{\vec{n}_1\cdot\vec{\Omega}<0} d\Omega \int_{\mathcal{F}_1} ds\ \sigma_{t1} \left|\vec{n}_1 \cdot \vec{\Omega}\right| \left(\psi_1 - \psi_1^{\text{inc}}\right)$$
$$+ \oint_{4\pi} d\Omega \int_{\mathcal{D}_2} dV\ \sigma_{t2}((L_2 - S_2)\psi_2 - q_2) + \int_{\vec{n}_2\cdot\vec{\Omega}<0} d\Omega \int_{\mathcal{F}_2} ds\ \sigma_{t2} \left|\vec{n}_2 \cdot \vec{\Omega}\right| \left(\psi_2 - \psi_2^{\text{inc}}\right)$$
$$+ \int_{\vec{n}_1\cdot\vec{\Omega}<0} d\Omega \int_{\mathcal{F}_l} ds\ \sigma_{t1} \left|\vec{n}_1 \cdot \vec{\Omega}\right| (\psi_1 - \psi_2) + \int_{\vec{n}_2\cdot\vec{\Omega}<0} d\Omega \int_{\mathcal{F}_r} ds\ \sigma_{t2} \left|\vec{n}_2 \cdot \vec{\Omega}\right| (\psi_2 - \psi_1) = 0. \tag{13}$$

Defining the incoming and outgoing currents on a subdomain as

$$j_{\text{i}}^{\text{in}}(\vec{r}) := \int_{\vec{n}_{\text{i}}\cdot\vec{\Omega}<0} d\Omega\ \left|\vec{n}_{\text{i}} \cdot \vec{\Omega}\right| \psi_{\text{i}} \quad \text{and} \quad j_{\text{i}}^{\text{out}}(\vec{r}) := \int_{\vec{n}_{\text{i}}\cdot\vec{\Omega}>0} d\Omega\ \left|\vec{n}_{\text{i}} \cdot \vec{\Omega}\right| \psi_{\text{i}}, \tag{14}$$

we then can write

$$\oint_{4\pi} d\Omega \int_{\mathcal{D}_{\text{i}}} dV\ (L_{\text{i}}\psi_{\text{i}} - S_{\text{i}}\psi_{\text{i}} - q_{\text{i}}) = \oint_{\partial\mathcal{D}_{\text{i}}} ds\ (j_{\text{i}}^{\text{out}} - j_{\text{i}}^{\text{in}}) + \int_{\mathcal{D}_{\text{i}}} dV\ (\sigma_{\text{ai}}\phi_{\text{i}} - Q_{\text{i}}). \tag{15}$$

Using Eq. (15) in Eq. (13), we get

$$\begin{aligned}
&\sigma_{\mathrm{t}1}\left(\int_{\mathcal{F}_1}+\int_{\mathcal{F}_\mathrm{l}}\right) ds\ (j_1^{\mathrm{out}}-\cancel{j_1^{\mathrm{in}}})+\sigma_{\mathrm{t}1}\int_{\mathcal{D}_1} dV\ (\sigma_{\mathrm{a}1}\phi_1-Q_1)\\
&\qquad +\sigma_{\mathrm{t}2}\left(\int_{\mathcal{F}_2}+\int_{\mathcal{F}_\mathrm{r}}\right) ds\ (j_2^{\mathrm{out}}-\cancel{j_2^{\mathrm{in}}})+\sigma_{\mathrm{t}2}\int_{\mathcal{D}_2} dV\ (\sigma_{\mathrm{a}1}\phi_2-Q_2)\\
&+\sigma_{\mathrm{t}1}\left(\int_{\mathcal{D}_1}+\int_{\mathcal{F}_\mathrm{l}}\right) ds\,\cancel{j_1^{\mathrm{in}}}-\sigma_{\mathrm{t}1}\int_{\mathcal{F}_1} ds\int_{\vec{n}_1\cdot\vec{\Omega}<0} d\Omega\ \left|\vec{n}_1\cdot\vec{\Omega}\right|\psi_1^{\mathrm{inc}}-\sigma_{\mathrm{t}1}\int_{\mathcal{F}_\mathrm{l}}\int_{\vec{n}_1\cdot\vec{\Omega}<0}\left|\vec{n}_1\cdot\vec{\Omega}\right|\psi_2(\mathcal{F}_\mathrm{r})\\
&+\sigma_{\mathrm{t}2}\left(\int_{\mathcal{D}_2}+\int_{\mathcal{F}_\mathrm{r}}\right) ds\,\cancel{j_2^{\mathrm{in}}}-\sigma_{\mathrm{t}1}\int_{\mathcal{F}_2} ds\int_{\vec{n}_2\cdot\vec{\Omega}<0} d\Omega\ \left|\vec{n}_2\cdot\vec{\Omega}\right|\psi_2^{\mathrm{inc}}-\sigma_{\mathrm{t}2}\int_{\mathcal{F}_\mathrm{r}}\int_{\vec{n}_2\cdot\vec{\Omega}<0}\left|\vec{n}_2\cdot\vec{\Omega}\right|\psi_1(\mathcal{F}_\mathrm{l})=0,
\end{aligned}\tag{16}$$

where the incoming currents that sum to zero have been crossed out.

Denoting balances of $\mathcal{D}_1$ and $\mathcal{D}_2$ by $\mathbf{B}_1$ and $\mathbf{B}_2$, respectively, we then have a weighted balance equation:

$$\sigma_{\mathrm{t}1}\mathbf{B}_1+\sigma_{\mathrm{t}2}\mathbf{B}_2=0,\tag{17}$$

where

$$\begin{aligned}
\mathbf{B}_1=&\left(\int_{\mathcal{F}_1}+\int_{\mathcal{F}_\mathrm{l}}\right) ds\ j_1^{\mathrm{out}}+\int_{\mathcal{D}_1} dV\ (\sigma_{\mathrm{a}1}\phi_1-Q_1)\\
&-\int_{\mathcal{F}_1} ds\int_{\vec{n}_1\cdot\vec{\Omega}<0} d\Omega\ \left|\vec{n}_1\cdot\vec{\Omega}\right|\psi_1^{\mathrm{inc}}-\int_{\mathcal{F}_\mathrm{l}} ds\int_{\vec{n}_1\cdot\vec{\Omega}<0} d\Omega\ \left|\vec{n}_1\cdot\vec{\Omega}\right|\psi_2(\mathcal{F}_\mathrm{r}),
\end{aligned}\tag{18}$$

and

$$\begin{aligned}
\mathbf{B}_2=&\left(\int_{\mathcal{F}_2}+\int_{\mathcal{F}_\mathrm{r}}\right) ds\ j_2^{\mathrm{out}}+\int_{\mathcal{D}_2} dV\ (\sigma_{\mathrm{a}2}\phi_2-Q_2)\\
&-\int_{\mathcal{F}_2} ds\int_{\vec{n}_2\cdot\vec{\Omega}<0} d\Omega\ \left|\vec{n}_2\cdot\vec{\Omega}\right|\psi_2^{\mathrm{inc}}-\int_{\mathcal{F}_\mathrm{r}} ds\int_{\vec{n}_2\cdot\vec{\Omega}<0} d\Omega\ \left|\vec{n}_2\cdot\vec{\Omega}\right|\psi_1(\mathcal{F}_\mathrm{l}).
\end{aligned}\tag{19}$$

For all nonzero $\sigma_{\mathrm{t}1}$ and $\sigma_{\mathrm{t}2}$, in order to make Eq. (17) true, one must have conservation in each subdomain:

$$\mathbf{B}_1\equiv 0\quad\text{and}\quad\mathbf{B}_2\equiv 0.\tag{20}$$

Additionally, this implies that there is global conservation because $\mathbf{B}_1 + \mathbf{B}_2 = 0$. Therefore, the SDLS scheme is conservative if the cross section is subdomain-wise constant (and nonzero).

4. Numerical results

The implementation is carried out by the `C++` finite element library `deal.II` [17]. In all tests, we also include results from solving the globally conservative self-adjoint angular flux (SAAF) equation with CFEM as a comparison[2, 18]. In all problems, piecewise linear polynomial basis functions are used.

4.1. Modified Reed's problem

The first problem we solve is a modification of Reed's problem [19]. The material properties we use are listed in Table 1. Results using S_8 in angle are presented in Figure 2. In this figure 48 cells are used for CFEM-LS (green line), CFEM-SAAF (blue line) and SDLS (red lines) calculations. For SDLS, the interfaces are set at $x = 3, 5, 6$ cm.

The reference solution (black dash line) is made from CFEM-SAAF with 8×10^3 cells. Without enough refinement, solutions for CFEM-SAAF and CFEM-LS are distorted in the thin absorber ($x \in (3, 5)$ cm). Also, the accuracy in the source region $x \in (2, 3)$ cm suffers. However, SDLS, through adding a few extra DoFs on the material interfaces and therefore introducing discontinuities, provides much better agreement with the reference using merely 48 cells plus 3 extra degrees of freedom per direction.

Table 1: Material configuration for modified Reed's problem.

x [cm]	(0,2)	(2,3)	(3,5)	(5,6)	(6,8)
σ_t [cm^{-1}]	1	1	0.005	5	50
σ_s [cm^{-1}]	0.9	0.9	0	0	0
Q	0	1	0	0	50

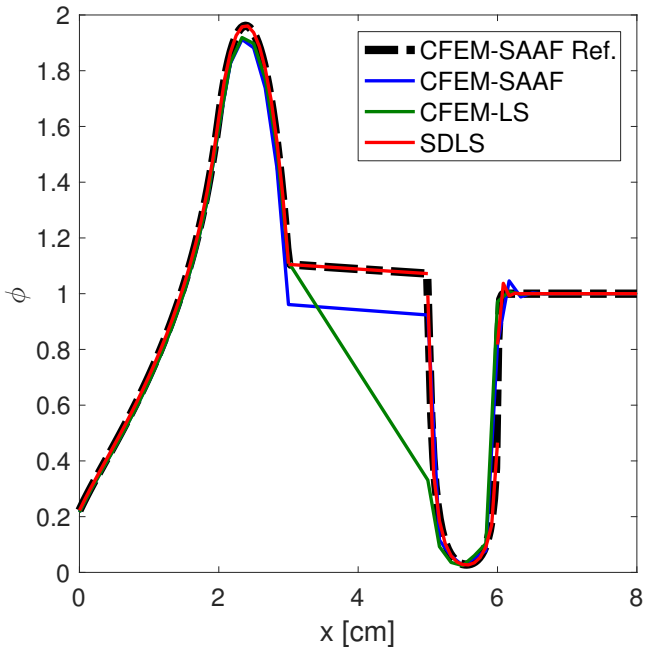

Figure 2: Modified Reed's problem result comparison.

4.2. Two region absorption problem

The second test problem is a 1D slab pure absorber problem. There is a unit incident angular flux on left boundary of the slab. No source appears in the domain. In this problem

$$\sigma_{\mathrm{t}} = \begin{cases} 0.1\,\mathrm{cm}^{-1} & x < 1\,\mathrm{cm} \\ 10\,\mathrm{cm}^{-1} & \text{otherwise} \end{cases}.$$

The reference solution in this problem was computed with first order S_8 using diamond difference with 2×10^4 cells in space.

The results in Figure 3 compare coarse solutions using different methods. The LS and SAAF solutions in the thin region are affected by the presence of the thick region, even though that region is downstream of the incoming boundary source. Increasing the cell count does improve these solutions, but there is still significant discrepancy with the reference solution. In both cases,

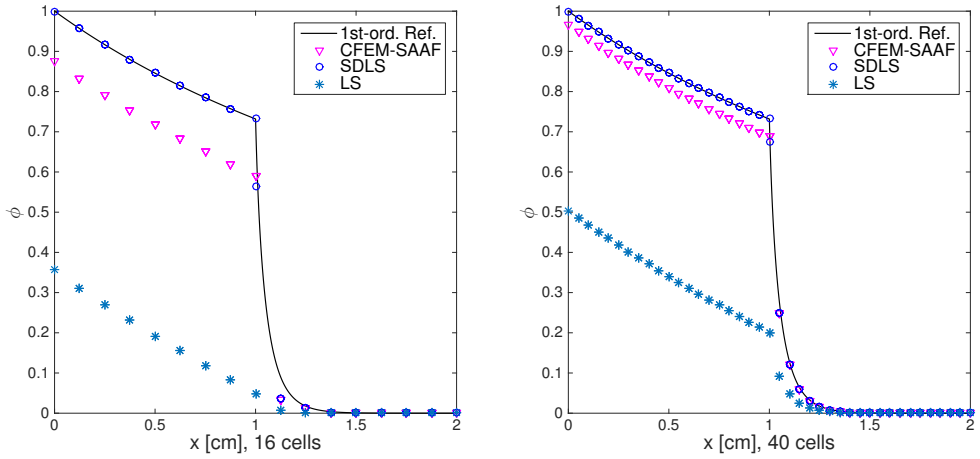

(a) 16 cells. (b) 40 cells.

Figure 3: Two-region absorption results comparison with LS, SAAF and SDLS.

the SDLS solution captures the behavior of the reference solution. In Figure 4 we see that both LS SDLS and SAAF converge to the exact solution at second-order, with the convergence for LS being a bit more erratic.

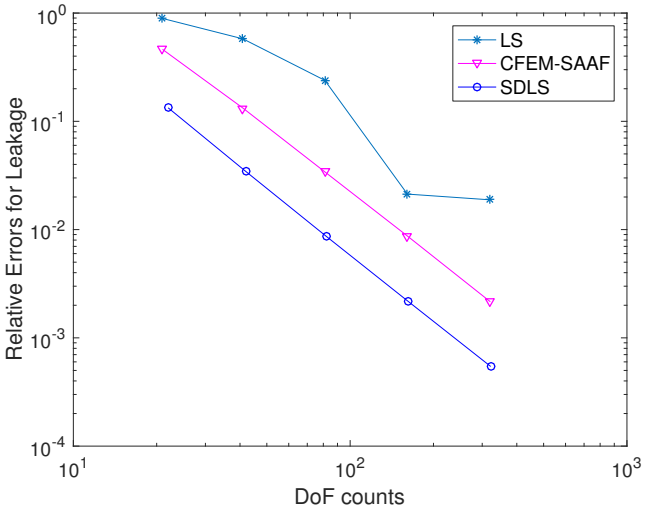

Figure 4: Leakage errors at right boundary.

Table 2 presents the relative global balances for different methods defined as

$$\mathbf{B}_{\text{rel}} = \frac{|\mathbf{B}|}{\int\limits_{\vec{n}\cdot\vec{\Omega}<0} d\Omega \int\limits_{\partial\mathcal{D}} ds \ \left|\vec{n}\cdot\vec{\Omega}\right| \psi^{\text{inc}} + \int\limits_{\mathcal{D}} dV \ Q}.$$

As expected, LS presents large balance errors, even when the mesh is refined. On the other hand, CFEM-SAAF and SDLS give round-off balance to the iterative solver tolerance as expected.

Table 2: Relative global balance with different methods.

Number of Cells	20	40	80	160	320
LS	8.439×10^{-1}	6.426×10^{-1}	3.564×10^{-1}	3.430×10^{-1}	4.948×10^{-2}
CFEM-SAAF	5.899×10^{-14}	1.786×10^{-13}	2.615×10^{-13}	1.274×10^{-12}	5.599×10^{-12}
SDLS	2.148×10^{-13}	7.668×10^{-13}	1.492×10^{-12}	2.090×10^{-11}	2.704×10^{-12}

4.3. One group iron-water problem

The last test is a modified one-group iron-water shielding problem [20] used to test accuracy of numerical schemes in relatively thick materials (see the configuration in Figure 5a). Material properties listed in Table 3 are from the thermal group data in [20]. S_4 is used as the angular discretization. The reference is CFEM-SAAF using 1200×1200 cells (see the scalar flux in Figure 5b). The scalar flux in the domain is rather smooth due to the scatterings. As a result, with moderately fine mesh (120×120 cells), we see SDLS graphically agrees with SAAF and LS in the line-out illustrated in Figure 6a. We further examine the absorption rate error in iron. As shown in Figure 6b, LS and SAAF presents similar spatial convergence rates. However, LS presents lower accuracy than CFEM-SAAF with the presence of material interface between iron and water. On the other hand, by setting two interfaces between iron and water and introducing extra DoFs on the interfaces, SDLS converges to the reference solution much earlier that than the other methods.

Table 3: Material cross sections in one-group iron-water test.

Materials	σ_{t} [cm^{-1}]	σ_{s} [cm^{-1}]
Water	3.2759	3.2656
Iron	1.1228	0.9328

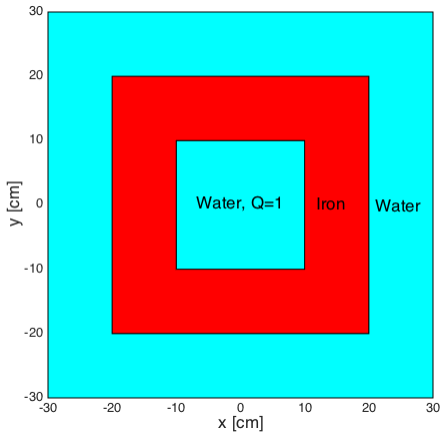

(a) Problem configuration.

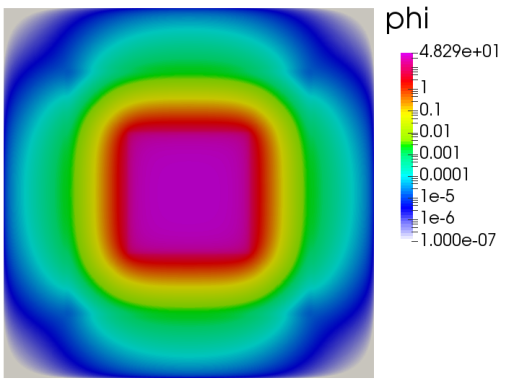

(b) Scalar flux distribution from reference.

Figure 5: Results from the iron water problem.

5. Concluding remarks and future work

In this work, we proposed a subdomain discontinuous least-squares discretization method for solving neutron particle transport. It solves a least-squares problem on each region of the problem that has the same total cross-section, and couples the contiguous regions with discontinuous interface conditions. We demonstrated that our formulation preserves conservation in each subdomain and gives smaller numerical error than either SAAF or standard least squares methods.

Though SDLS is angularly discretized with S_N method, P_N would be applicable in the angular discretization as well. Therein, LSP_N[21, 22, 23] is applied in each subdomain with Mark-type boundary condition used as interface condition. Further, since SDLS allows the discontinuity on the subdomain interface,

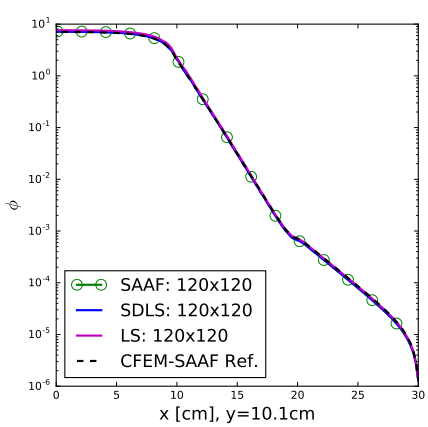

(a) Line-out plot for $x = 10.1$ cm.

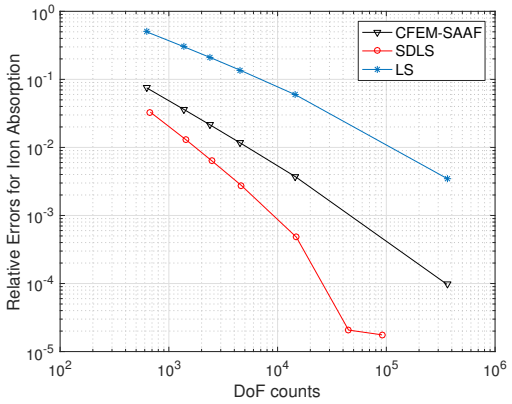

(b) Relative errors of absorption rate in iron vs DoF counts in one direction.

Figure 6: Results from the iron water problem.

different angular schemes, e.g. S_N and P_N can be used in different subdomains. In fact, with borrowing the interface discontinuity methodology, the angular hybridization has been implemented for SAAF[24, 25].

Acknowledgements

W. Zheng is thankful to Dr. Bruno Turksin from Oak Ridge National Laboratory for the suggestions on multi-D implementation. Also, Zheng appreciates Dr. Yaqi Wang from Idaho National Laboratory for his suggestions to make the notation simple and clear.

This project is funded by Department of Energy NEUP research grant from Battelle Energy Alliance, LLC- Idaho National Laboratory, Contract No: C12-00281.

References

References

[1] M. L. Adams, Discontinuous finite element transport solutions in thick diffusive problems, Nuclear Science and Engineering 137 (3) (2001) 298–

333.

[2] J. E. Morel, J. M. McGhee, A Self-Adjoint Angular Flux Equation, Nuclear Science and Engineering 132 (3) (1999) 312–325.

[3] C. J. Gesh, Finite element methods for second order forms of the transport equation, PhD dissertation, Texas A&M University (1999).

[4] C. J. Gesh, M. L. Adams, Finite Element Solutions of Second-order Forms of the Transport Equation at the Interface Between Diffusive and Non-Diffusive Regions, in: M&C 2001, 2001, salt Lake City, Utah, United States.

[5] Y. Zhang, Even-parity S_N Adjoint Method Including SP_N Model Error and Iterative Efficiency, Ph.D. dissertation, Texas A&M University (2014).

[6] W. Zheng, Least-squares and other residual based techniques for radiation transport calculations, PhD dissertation, Texas A&M University (2016).

[7] J. Hansen, J. Peterson, J. Morel, J. E. Ragusa, Y. Wang, A Least-Squares Transport Equation Compatible with Voids, Journal of Computational and Theoretical Transport 43 (1-7) (2015) 374–401.

[8] Non-oscillatory and non-diffusive solution of convection problems by the iteratively reweighted least-square finite element method, Journal of Computational Physics 105 (1993) 108 – 121.

[9] On the numerical solution of conservation laws by minimizing residuals, Journal of Computational Physics 113 (2) (1994) 304 – 308.

[10] J. L. Guermond, A finite element technique for solving first order pdes in l_p, SIAM J. Numer. Anal 42 (2) (2004) 714–737.

[11] W. Zheng, R. G. McClarren, Non-oscillatory Reweighted Least Square Finite Element Method for S_N Transport, in: ANS Winter Meeting 2015, Vol. 113, pp. 688–691.

[12] W. Zheng, R. G. McClarren, Non-oscillatory Reweighted Least Square Finite Element for Solving P_N Transport, in: ANS Winter Meeting 2015, Vol. 113, pp. 692–695.

[13] C. Drumm, Spherical harmonics (P_n) methods in the sceptre radiation transport code, in: ANS MC2015 - Joint International Conference on Mathematics and Computation (M&C), Supercomputing in Nuclear Applications (SNA) and the Monte Carlo (MC) Method, 2015, nashville, TN, United States.

[14] V. M. Laboure, R. G. McClarren, Y. Wang, Globally Conservative, Hybrid Self-Adjoint Angular Flux and Least-Squares Method Compatible with Void, ArXiv e-prints`arXiv:1605.05388`.

[15] J. R. Peterson, H. R. Hammer, J. E. Morel, J. C. Ragusa, Y. Wang, Conservative Nonlinear Diffusion Acceleration Applied to the Unweighted Least-squares Transport Equation in MOOSE, in: ANS MC2015 - Joint International Conference on Mathematics and Computation (M&C), Supercomputing in Nuclear Applications (SNA) and the Monte Carlo (MC) Method, 2015, nashville, TN, United States.

[16] R. Lin, Discontinuous Discretization for Least-Squares Formulation of Singularity Perturbed Reaction-Diffusion Problems in One and Two Dimensions, SIAM J. NUMER. ANAL 47 (1) (2008) 89–108.

[17] W. Bangerth, T. Heister, L. Heltai, G. Kanschat, M. Kronbichler, M. Maier, B. Turcksin, T. D. Young, The `deal.II` library, version 8.2, Archive of Numerical Software 3.

[18] Y. Wang, H. Zhang, R. C. Martineau, Diffusion Acceleration Schemes for Self-Adjoint Angular Flux Formulation with a Void Treatment, Nuclear Science and Engineering 176 (2) (2014) 201–225.

[19] W. Reed, New difference schemes for the neutron transport equation, Nucl. Sci. Eng. 46: No. 2, 309-14.

[20] C. L. Castrianni, M. L. Adams, A Nonlinear Corner-Balance Spatial Discretization for Transport on Arbitrary Grids, Nuclear Science and Engineering 128 (3) (1998) 278–296.

[21] W. Zheng, R. G. McClarren, Accurate Least-Squares PN Scaling based on Problem Optical Thickness for solving Neutron Transport Problems, Progress in Nuclear Energy (submitted on Sept. 2016).

[22] T. A. Manteuffel, K. J. Ressel, Least-Squares Finite-Element Solution of the Nuetron Transport Equation in Diffusive Regimes, SIAM J. Numer. Anal 35 (2) (1998) 806–835.

[23] E. Varin, G. Samba, Spherical Harmonics Finite Element Transport Equation Solution Using a Least-Square Approach, Nuclear Science and Engineering 151 (2005) 167–183.

[24] S. Schunert, Y. Wang, M. D. DeHart, R. C. Martineau, Hybrid P_N-S_N Calculations with SAAF for the Multiscale Transport Capability in Rattlesnake, in: PHYSOR 2016.

[25] Y. Wang, S. Schunert, M. DeHart, R. Matineau, W. Zheng, Hybrid P_N-S_N With Lagrange Multiplier and Upwinding for the Multiscale Transport Capability in Rattlesnake, Progress in Nuclear Energy (submitted on Sept. 2016).